

Persisting Meissner state and incommensurate phases of hard-core boson ladders in a flux

M. Di Dio,¹ S. De Palo,^{1,2} E. Orignac,³ R. Citro,⁴ and M.-L. Chiofalo⁵

¹*CNR-IOM-Democritos National Simulation Centre, UDS Via Bonomea 265, I-34136, Trieste, Italy*

²*Dipartimento di Fisica Teorica, Università di Trieste, Trieste, Italy*

³*Laboratoire de Physique de l'École Normale Supérieure de Lyon,*

CNRS UMR5672, 46 Allée d'Italie, F-69364 Lyon Cedex 7, France

⁴*Dipartimento di Fisica "E.R. Caianiello", Università degli Studi di Salerno and Unità Spin-CNR ,
Via Giovanni Paolo II, 132, I-84084 Fisciano (Sa), Italy*

⁵*Dept. of Physics "Enrico Fermi" and INFN, Università di Pisa Largo Bruno Pontecorvo 3 I-56127 Pisa, Italy*
(Dated: April 13, 2021)

The phase diagram of a half-filled hard core boson two-leg ladder in a flux is investigated by means of numerical simulations based on the Density Matrix Renormalization Group (DMRG) algorithm and bosonization. We calculate experimentally accessible observables such as the momentum distribution, as well as rung current, density wave and bond-order wave correlation functions, allowing us to identify the Mott Meissner and Mott Vortex states. We follow the transition from commensurate Meissner to incommensurate Vortex state at increasing interchain hopping till the critical value [Piraud *et al.* Phys. Rev. B **91**, 140406 (2015)] above which the Meissner state is stable at any flux. For flux close to π , and below the critical hopping, we observe the formation of a second incommensuration in the Mott Vortex state that could be detectable in current experiments.

PACS numbers: 03.75.Lm,05.30.Rt,64.70.Rh,71.10.Pm

Superconductors in external magnetic field $H < H_{c1}$ exhibit the Meissner-Ochsenfeld effect where surface currents screen completely the magnetic field in the bulk, resulting in perfect diamagnetism [1]. Type-I superconductors return to the normal state for $H > H_{c1}$ while in type-II superconductors, for $H_{c1} < H < H_{c2}$ a vortex phase is formed, in which the magnetic field partially penetrates the system along flux lines surrounded by screening currents. This behavior can be understood in the framework of spontaneous breaking of a global U(1) symmetry via the Landau-Ginzburg equation[1]. In a quasi-one dimensional system, such symmetry breaking is precluded by the Mermin-Wagner-Hohenberg theorem[2, 3]. However, in the case of a bosonic two-leg ladder [4, 6, 14], an analog of the Meissner phase was predicted to exist in the ground state for low flux, while for higher flux a Tomonaga-Luttinger liquid (TLL) of vortices was expected. The quantum phase transition between these two states is in the commensurate-incommensurate (C-IC) universality class [15, 16]. Other orderings have been predicted, such as chiral superfluid order at half a flux quantum per plaquette [4, 9, 10] and a chiral Mott insulating phase[11–15], which is a Mott regime[16] possessing chiral currents as well as a spin-density wave phase. DMRG studies of ladders with diagonal interchain hopping are also available [17–22]. While the original proposal was made in the context of Josephson junction ladders, where the quantum effects are spoiled by dissipation [23], the advent of ultracold atomic gases offers another realization of strongly interacting one dimensional boson systems[24, 25]. Moreover, it has been shown theoretically [26, 27] and experimentally [28] how artificial gauge field could be created in these systems. Recently,

the transition from Meissner to Vortex phases in non-interacting bosonic ladders of ultracold atoms has been studied experimentally at fixed flux $\pi/2$ per plaquette and variable interleg hopping [29].

In this Letter we explore the phase diagram of hard-core spinless bosons on a two-leg ladder at half-filling as a function of flux and interchain hopping by means of numerical simulations using DMRG algorithm and bosonization. We find, in agreement with [30], that hard-core constraints cause a significant enlargement of the Meissner phase over the vortex one with respect to the non-interacting case: above a critical value of the interchain hopping[30] the system remains in the Mott-Meissner (MM) state for any flux (see Fig. 1). Below the critical interchain hopping, both the behavior of the momentum distribution and of the rung current, show that the transition from Mott-Meissner (MM) to Mott-Vortex (MV) state falls in the universality class of the C-IC transition[14]. For fluxes close to π , we observe another incommensuration, whose origin is discussed within bosonization.

We consider[14] a two-component system of hard core bosons on two leg ladder, with a flux per plaquette λ and interchain hopping Ω :

$$H_\lambda = -t \sum_{j,\sigma} \left(b_{j,\sigma}^\dagger e^{i\lambda\sigma} b_{j+1,\sigma} + \text{H.c.} \right) + \Omega \sum_j \left(b_{j,\uparrow}^\dagger b_{j,\downarrow} + \text{H.c.} \right), \quad (1)$$

with $b_{j,\sigma}^\dagger$ ($b_{j,\sigma}$) bosonic creation (annihilation) operator at site j , $\sigma = \pm 1/2$ the chain index, and $te^{i\lambda\sigma}$ the hopping amplitude along the chain σ . This Hamiltonian can be

mapped onto a system of spin-1/2 [31] bosons with spin-orbit coupling in a transverse magnetic field [32] with each spinor state corresponding to one leg of the ladder. For half-filling, i.e. for one boson per rung, at $\lambda = 0$ and $\Omega \neq 0$ the ground state of (1) is a rung-Mott Insulator[5]. For $\lambda > 0$, according to the bosonization treatment[3], two phases with a charge gap are expected[13, 14, 14, 15], the Mott-Meissner (MM) and the Mott-Vortex (MV) state. In the MM state, for $0 < \lambda < \lambda_c$, two currents of opposite sign flow along the legs[30], the interchain current

$$J_r(l) = i\Omega \left(b_{l,\uparrow}^\dagger b_{l,\downarrow} - b_{l,\downarrow}^\dagger b_{l,\uparrow} \right) \quad (2)$$

has zero expectation value and exponentially decaying correlations, and the screening current, *i.e.* the difference between the currents of the two legs

$$J_s = -it \sum_{j,\sigma} \left(\sigma e^{i\lambda\sigma} b_{j,\sigma}^\dagger b_{j+1,\sigma} - \sigma e^{-i\lambda\sigma} b_{j+1,\sigma}^\dagger b_{j,\sigma} \right), \quad (3)$$

is a smooth function of the applied flux (increasing linearly at small flux). On increasing the flux $\lambda > \lambda_c(\Omega)$, the system enters the MV state, there is a sudden drop[30] of the screening current J_s and simultaneously the rung current correlations decay becomes algebraic[30] with an incommensurate modulation of wavevector $q(\lambda)$. Close to the transition point $\lambda_c(\Omega)$, the wavevector $q(\lambda) \sim \sqrt{\lambda^2 - \lambda_c^2}$. In the non-interacting case, the Hamiltonian Eq. (1) can be readily diagonalized[14, 16] and $\lambda_c^{(0)}(\Omega) = 2 \arctan[\Omega/(4t)]$. The occurrence of the MV phase can be seen out also in the total, as well as, in the spin resolved momentum distribution[6] of the system:

$$n(k) = \sum_{\sigma} n_{\sigma}(k) = \frac{1}{L} \sum_{\sigma} \sum_{i,j}^{L-1} e^{ik(r_i - r_j)} \langle b_{i,\sigma}^\dagger b_{j,\sigma} \rangle. \quad (4)$$

In the MM phase $n(k)$ has a single maximum at $k = 0$, whereas in the MV phase it exhibits a pair of maxima $k = \pm q(\lambda)/2$ [45]. We have obtained the ground state phase-diagram of (1) by computing various observables like the momentum distribution and the screening current J_s together with the Fourier Transform (FT) $C(k) = \sum_l e^{-ikl} \langle J_r(l) J_r(0) \rangle$ of the rung current correlation function.

While performing simulations with both periodic (PBC) and open (OBC) boundary conditions, we found the former to be more suitable for our system, despite the well-known computationally more demanding convergence properties typical of PBC [35–37]. As such we run simulations employing PBC for system sizes ranging from $L = 16$ to $L = 64$, keeping up to $m = 1256$ states during the renormalization procedure. In this way the truncation error *i.e.* the weight of the discarded states, is at most of order 10^{-6} , while the maximum error on the

ground-state energy is of order 5×10^{-5} at its most. We further extrapolate in the limit $m \rightarrow \infty$ all the quantities calculated to characterize the phase diagram. In

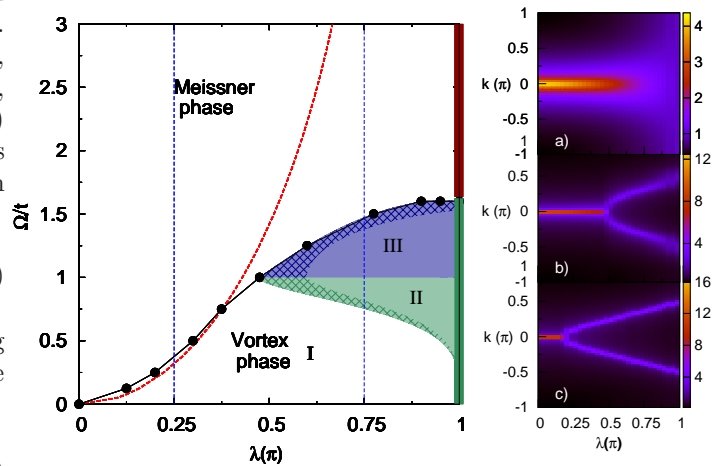


FIG. 1: (color online) Left panel: Phase diagram of (1) as a function of flux per plaquette λ and Ω/t . The phase boundary between the Meissner and the Vortex phase is shown by the black solid line, displaying the persistence of the Meissner phase[30] above the threshold $\Omega > \Omega_c$ for all fluxes λ , except $\lambda = \pi$. For comparison the red-dashed line shows the boundary $\lambda_c^{(0)}(\Omega)$ for the non-interacting system. In the shaded area a second incommensuration appears. In the green area (region II) extra peaks at $k = \pi$ develop in the FT of the rung current correlations and they become the dominant correlations in the blue region (III). The double line (green vs dark red) at $\lambda = \pi$ represents the transition to a localized phase. In the right panel we show intensity plots of $n(k)$ versus λ and k . In panel (a), at $\Omega/t = 1.75$ the system is always in the MM phase, indeed only a single maximum at $k = 0$ is visible for all λ . At $\lambda = \pi$, $n(k) = 1$ indicating the formation of a fully localized state (dark red solid line). In panel (b) and (c), for $\Omega/t = 1$ and 0.25 respectively, the transition from MM to the MV with two maxima symmetric around $k = 0$, is shown.

Fig. 1, we summarize our findings for the phase diagram at half-filling. At variance with the non-interacting case where there is a critical $\lambda_c^{(0)}(\Omega)$ for all Ω , in the presence of the hard-core interaction, for interchain hoppings $\Omega > \Omega_c$, the commensurate-incommensurate transition disappears[30] and the MM phase is stable for all fluxes. Another effect of the hard-core interaction, as we will discuss below, is that in the Vortex phase, at $\lambda = \pi$ and λ close to π , a commensurate peak appears in $C(k \simeq \pi)$, along with an incommensuration in the density correlations. At $\lambda = \pi$, and for $\Omega > \Omega_c$ a fully rung localized phase is obtained. Such rung localized ground state was discussed in the limit $\Omega \gg t$ in [30].

We have characterized the nature of the Mott-Meissner and Mott-Vortex phases by examining $C(k)$, the staggered boson density wave $S(k)$ and the symmetric bond-order wave S_{BOW}^c static structure factors which bring information on the spin density and bond-order waves,

respectively:

$$S(k) = \frac{1}{L} \sum_{\substack{j,l=0 \\ \sigma\sigma'}}^{L-1} e^{ik(j-l)} \text{sign}(\sigma\sigma') \langle n_{j,\sigma} n_{l,\sigma'} \rangle, \quad (5)$$

$$S_{BOW}^c(k) = \frac{1}{L} \sum_{j,l=0}^{L-1} e^{ik(j-l)} \langle \delta B_j \delta B_l \rangle; \quad (6)$$

where $B_j = \sum_{\sigma} b_{j+1,\sigma}^\dagger b_{j,\sigma} + H.c.$ and $\delta B_j = B_j - \langle B_j \rangle$.

In Fig. 2 we follow the the MM–MV phase transition at small λ and Ω (see cut one in Fig.1). As predicted from bosonization [32] the vortex phase is signalled by the appearance in $C(k)$ of two cusp-like peaks respectively at $k = q(\lambda)$ and $k = 2\pi - q(\lambda)$ (see panel a) of Fig. 2 whose heights do not scale with the size of the system (see Fig. 1 of [32]). In MV phase, the spin resolved momentum distribution $n_{\sigma}(k)$ shows a symmetric peak centered at $k = \sigma q(\lambda)$, as predicted by bosonization. In this region of parameter space the correlation length associated with the Mott gap[5] is comparable with the system size, and the peak takes a cusp-like shape as in a Tomonaga-Luttinger liquid[31], instead of the typical Lorentzian-shape expected for a Mott-insulator. Also $S(k)$ shows the expected low momentum behaviour

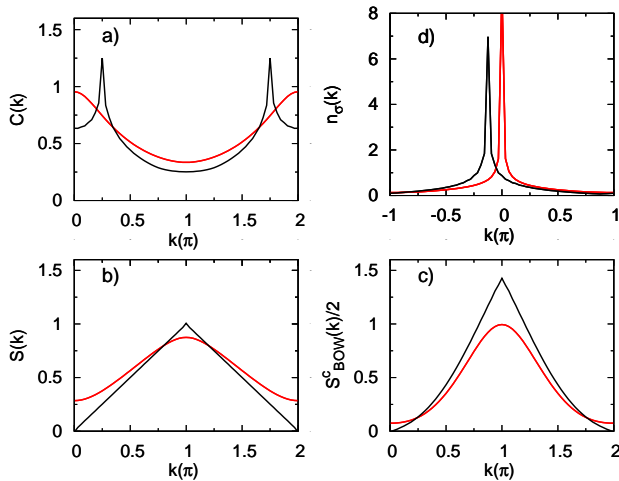


FIG. 2: We show FT of correlation functions as from DMRG simulation for $L = 64$ at $\lambda = \pi/4$ for two different values of the $\Omega/t = 0.0625$ and 1 , respectively in the Vortex (black solid line) and Meissner phase (red solid line). Panel a) shows the FT of the rung-current correlation function $C(k)$, panel b) the spin correlation functions $S(k)$ and panel c) the charge bond-order correlation function S_{BOW}^c . In panel d) the spin resolved momentum distribution is shown, with $n_{-\sigma}(k) = n_{\sigma}(-k)$.

according to bosonization approach: in the MM phase $S(k) = S(0) + ak^2 + o(k^2)$, with $S(0) > 0$, while in the MV phase $S(k) = \frac{K_s^* |k|}{\pi} + o(k)$, with $K_s^* = 1$ (as expected for a hard-core boson system) a signature of a TLL of

vortices. The transition is also seen in $S(k \simeq \pi)$. In the MM phase, $S(k \simeq \pi)$ shows a Lorentzian-shaped peak while in the MV phase this peak takes a cusp-like shape. A similar change across the MM-MV transition is also seen in the correlation function $S_{BOWc}(k \simeq \pi)$ (see Supplemental Material[32]). This description breaks down

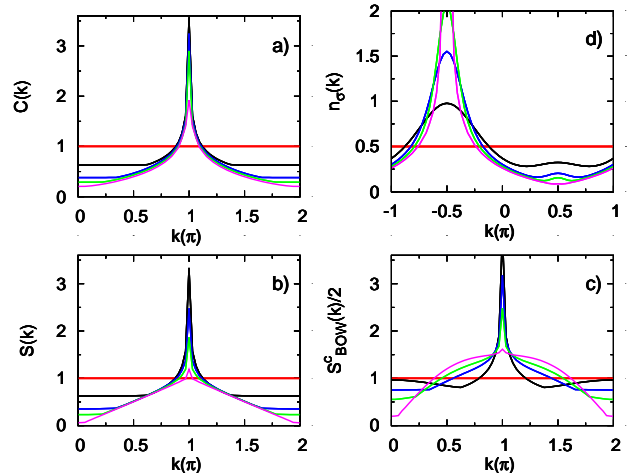


FIG. 3: We show FT of correlation functions as from DMRG simulations for $L = 64$ at $\lambda = \pi$ at various Ω/t . Panel a) shows the FT of the rung-current correlation function $C(k)$, panel b) the spin correlation function $S(k)$ and panel c) the charge bond-order correlation function S_{BOW}^c . In panel d) the spin resolved momentum distribution is shown. Red solid curves are for $\Omega/t = 1.75$ in the fully localised state, while black, blue, green and magenta solid lines are respectively for $\Omega/t = 1.5, 1.25, 1$ and 0.5 .

when λ is no longer a small quantity as $q(\lambda)$ would be comparable to the momentum cutoff.

At $\lambda = \pi$ the major changes from the conventional C-IC transition at small flux are observed. To derive the low energy Hamiltonian it becomes necessary to choose the gauge with the vector potential along the rungs of the ladder, so that the interchain hopping reads:

$$H_{hop.} = \Omega \sum_{j,\sigma} (-)^j b_{j,\sigma}^\dagger b_{j,-\sigma}. \quad (7)$$

After applying bosonization, the hopping Hamiltonian can be rewritten in terms of a free boson ϕ_c describing the total density fluctuations coupled to $SU(2)_1$ Wess-Zumino-Novikov-Witten (WZNW) currents $\mathbf{J}_{R,L}$ describing the chain antisymmetric density fluctuations by a term $\propto \Omega \cos \sqrt{2} \phi_c (J_R^y + J_L^y)$ (see [32] for details). Such a term can be treated in mean-field theory[20–23]. This procedure leads to an effective Hamiltonian with a gap $\Delta_c \sim \Omega^2$ for the total density excitations, while the antisymmetric density modes remain gapless and develop an incommensuration of wavevector $p(\Omega) \propto \Omega^2$ (see Fig. 2 in [32]). The presence of this predicted incommensuration is visible in the low momentum behaviour of $S(k)$

and $C(k)$ (panel a) and panel b) of Fig. 3 that become $\propto \frac{K^*}{2\pi} (|k-p(\Omega)| + |k+p(\Omega)|)$, *i.e.* constant for $|k| < p(\Omega)$ and linear in k for $|k| > p(\Omega)$. In the $S_{BOW}^c(k)$ we observe a cusp at the same vectors $p(\Omega)$ (panel c) of Fig. 3). As expected, all these correlation functions also develop a peak at $k = \pi/a$. A sign of the incommensurability at $\lambda = \pi$ should be visible also in the momentum distribution $n_\sigma(k)$ (see Fig. 3, panel d)). In this case, a calculation based on non-abelian bosonization and operator product expansion, would lead to three Lorentzian-like peaks centered in $\pi/(2a)$ and $\pi/(2a) \pm p(\Omega)/2$. However, these peaks cannot be separated if the correlation length in real space $u_c/\Delta_c \sim \Omega^{-2}$ is shorter than the wavelength $2\pi/p(\Omega) \sim \Omega^{-2}$. In the numerical simulations, at $L = 64$ in PBC, (see Fig. 3) a broad peak is observed for $k = \frac{\pi}{2a}$.

When $\lambda \lesssim \pi$ (second cut in Fig.1) we can proceed analogously to the previous case and choose a gauge such that:

$$H = -t \sum_{j,\sigma} \left(b_{j,\sigma}^\dagger e^{i(\lambda-\pi)\sigma} b_{j+1,\sigma} + \text{H.c.} \right) + \Omega \sum_{j,\sigma} (-1)^j b_{j,\sigma}^\dagger b_{j,-\sigma}, \quad (8)$$

and define $\delta\lambda = (\lambda - \pi)$, so that the bosonized Hamiltonian contains the extra term $\delta\lambda(J_R^z - J_L^z)$. For this case, the Fourier transform of the rung current correlation will present peaks at $k = \frac{\pi}{a}$ and $k = \frac{\pi}{a} \pm \sqrt{p(\Omega)^2 + (\delta\lambda/a)^2}$. When $\delta\lambda$ is increased, these last two peaks become dominant, and we crossover to the behavior already discussed for weak λ . At $\lambda < \pi$ the $C(k)$ (see Fig. 4) shows, beside the peak at $k = \frac{\pi}{a}$, two peaks symmetric around $k = \frac{\pi}{a}$, in real space these last two oscillations exhibit an exponential decay for $\Omega/t > 1$ and a power law for $\Omega/t \leq 1$ (region III and II in Fig.1). The situation is reversed for the oscillation at $k = \frac{\pi}{a}$. At $\Omega/t = 1$ all oscillations, for systems with $L = 64$ in PBC, exhibit power law decay. The effect of this incommensuration can also be followed in the behaviour at small k of $S(k)$ that instead of being a constant value for $k < \sqrt{p(\Omega)^2 + (\delta\lambda/a)^2}$ shows a linear behaviour. In $S_{BOW}^c(k)$, for $\Omega/t \leq 1$ two symmetric peaks are present at $k = \pm q(\lambda)$. We checked that the phase is a single component Tomonaga-Luttinger liquid by computing the Von Neumann entropy at $\Omega/t = 1.5$ for $\lambda = 0.75\pi$ and 0.8125π and obtaining the expected logarithmic dependence with system size[30], ruling out a Chiral Mott insulator[13, 15] for $\lambda \lesssim \pi$. At general commensurate filling n and flux $\lambda = 2\pi n$, the incommensuration generating term becomes $-i\Omega e^{i\sqrt{2}\phi_c} (J_R^+ + J_L^-) + \text{H.c.}$, leading to density wave phases with incommensuration. Let us finish by noting that such incommensuration is specific of hard core boson systems. With less repulsive interactions, the term that gives rise to the vortex lattice state would be relevant[13, 15, 42], while stronger repulsion would make the term stabilizing the checkerboard density wave relevant. Adding a nearest neighbor intra-

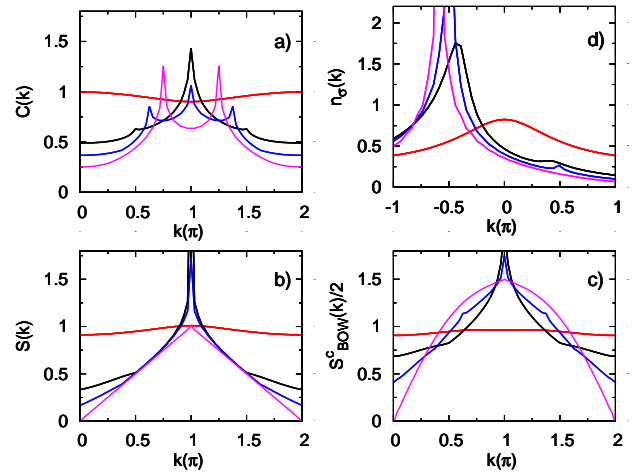


FIG. 4: We show FT of correlation functions as from DMRG simulations for $L = 64$ at $\lambda = 3\pi/4$ at various Ω/t . Panel a) shows the FT of the rung-current correlation function $C(k)$, panel b) the spin correlation function $S(k)$ and panel c) the symmetric bond-order correlation function S_{BOW}^c . In panel d) the chain resolved momentum distribution is shown, with $n_{-\sigma}(k) = n_\sigma(-k)$. Red solid curves are for $\Omega/t = 1.5$ in the Meissner phase, while black, blue, green and magenta solid lines are respectively for $\Omega/t = 1.25, 1$ and 0.625 .

chain interaction V to the hard core repulsion, a first phase transition at $V < 0$ will separate the vortex lattice from the incommensurate state, and a second transition at $V > 0$ will separate the incommensurate state from the density wave state.

In conclusion, we have studied a two-leg hard core boson ladder in an artificial gauge field. In contrast to the non-interacting case, the vortex phase is suppressed when the interchain hopping exceeds a threshold value, as found in [30]. At flux π per plaquette and $\Omega/t > 1.5$ the ground state becomes a tensor product of singly occupied rungs, as was expected[30] in the $\Omega/t \rightarrow \infty$ limit. For $\Omega/t < 1.5$, we have obtained an incommensurate insulating state similar to the spin-nematic state of frustrated XXZ spin chains[20–23]. In the case of a system of weakly coupled ladders, a long range ordered phase could form in which density wave or rung current would possess a long range commensurate order, but exponentially damped incommensurate correlations would still be present. The presented results could be detectable in current experiments with cold atoms[29] and the evidence of a persisting Meissner state could be relevant for quantum computing purposes in defining a stable flux qubit[43, 44].

We thank F. Ortolani for the DMRG code. Simulations were run at Università di Salerno and Università di Pisa local computing facilities. M.D.D. and M.L.C. acknowledge partial support from PRIN-2011 "Collective

Quantum Phenomena: from strongly correlated system to quantum simulators”.

-
- [1] M. Tinkham, *Introduction to Superconductivity* (McGraw Hill, New York, 1975).
- [2] N. D. Mermin and H. Wagner, Phys. Rev. Lett. **17**, 1133 (1967).
- [3] P. C. Hohenberg, Phys. Rev. **158**, 383 (1967).
- [4] M. Kardar, Phys. Rev. B **33**, 3125 (1986).
- [14] E. Orignac and T. Giamarchi, Phys. Rev. B **64**, 144515 (2001), cond-mat/0011497.
- [6] M.-C. Cha and J.-G. Shin, Phys. Rev. A **83**, 055602 (2011).
- [15] G. I. Japaridze and A. A. Nersesyan, JETP Lett. **27**, 334 (1978).
- [16] V. L. Pokrovsky and A. L. Talapov, Phys. Rev. Lett. **42**, 65 (1979).
- [9] E. Granato, Phys. Rev. B **42**, 4797 (1990).
- [10] Y. Nishiyama, Eur. Phys. J. B **17**, 295 (2000), cond-mat/0006311.
- [11] A. Dhar, M. Maji, T. Mishra, R. V. Pai, S. Mukerjee, and A. Paramekanti, Phys. Rev. A **85**, 041602 (2012).
- [12] A. Dhar, T. Mishra, M. Maji, R. V. Pai, S. Mukerjee, and A. Paramekanti, Phys. Rev. B **87**, 174501 (2013).
- [13] A. Petrescu and K. Le Hur, Phys. Rev. Lett. **111**, 150601 (2013).
- [14] A. Tokuno and A. Georges, New J. Phys. **16**, 073005 (2014).
- [15] A. Petrescu and K. Le Hur, Phys. Rev. B **91**, 054520 (2015).
- [16] A. Keleş and M. O. Oktel, Phys. Rev. A **91**, 013629 (2015).
- [17] J. Zhao, S. Hu, J. Chang, P. Zhang, and X. Wang, Phys. Rev. A **89**, 043611 (2014).
- [18] J. Zhao, S. Hu, J. Chang, F. Zheng, P. Zhang, and X. Wang, Phys. Rev. B **90**, 085117 (2014).
- [19] Z. Xu, W. Cole, and S. Zhang, Phys. Rev. A **89**, 051604(R) (2014), arXiv:1403.3491.
- [20] S. Peotta, L. Mazza, E. Vicari, M. Polini, R. Fazio, and D. Rossini, J. Stat. Mech.: Theor. Exp. **2014**, P09005 (2014).
- [21] M. Piraud, Z. Cai, I. P. McCulloch, and U. Schollwöck, Phys. Rev. A **89**, 063618 (2014).
- [22] L. Barbiero, M. Abad, and A. Recati, *Magnetic phase transition in coherently coupled bose gases in optical lattices*, arXiv:1403.4185 (2014).
- [23] R. Fazio and H. van der Zant, Phys. Rep. **355**, 235 (2001).
- [24] B. Paredes, A. Widera, V. Murg, O. Mandel, S. Fölling, I. Cirac, G. Shlyapnikov, T. Hansch, and I. Bloch, Nature (London) **429**, 277 (2004).
- [25] T. Kinoshita, T. Wenger, and D. Weiss, Science **305**, 5687 (2004).
- [26] K. Osterloh, M. Baig, L. Santos, P. Zoller, and M. Lewenstein, Phys. Rev. Lett. **95**, 010403 (2005).
- [27] J. Ruseckas, G. Juzeliūnas, P. Öhberg, and M. Fleischhauer, Phys. Rev. Lett. **95**, 010404 (2005).
- [28] Y. Lin, K. Jimenez-Garcia, and I. B. Spielman, Nature **471**, 83 (2011).
- [29] M. Atala, M. Aidelsburger, M. Lohse, J. Barreiro, B. Paredes, and I. Bloch, Nature Physics **10**, 588 (2014).
- [30] M. Piraud, F. Heidrich-Meisner, I. P. McCulloch, S. Greschner, T. Vekua, and U. Schollwöck, Phys. Rev. B **91**, 140406 (2015).
- [31] M. A. Cazalilla, R. Citro, T. Giamarchi, E. Orignac, and M. Rigol, Rev. Mod. Phys. **83**, 1405 (2011), arXiv:1101.5337.
- [32] M. Di Dio, S. De Palo, E. Orignac, R. Citro, and M.-L. Chiofalo, *Supplementary material for "persisting meissner state and ..."* (2015), see Supplemental Material at [URL will be inserted by publisher] for detailed bosonization calculation.
- [5] F. Crépin, N. Laflorencie, G. Roux, and P. Simon, Phys. Rev. B **84**, 054517 (2011).
- [3] F. D. M. Haldane, Phys. Rev. Lett. **47**, 1840 (1981).
- [35] S. R. White, Phys. Rev. Lett. **69**, 2863 (1992).
- [36] S. R. White, Phys. Rev. B **48**, 10345 (1993).
- [37] U. Schollwöck, Rev. Mod. Phys. **77**, 259 (2005).
- [20] A. A. Nersesyan, A. O. Gogolin, and F. H. L. Essler, Phys. Rev. Lett. **81**, 910 (1998).
- [21] P. Lecheminant, T. Jolicoeur, and P. Azaria, Phys. Rev. B **63**, 174426 (2001).
- [22] T. Jolicoeur and P. Lecheminant, Prog. Theor. Phys. Supp. **145**, 23 (2002).
- [23] M. Zarea, M. Fabrizio, and A. Nersesyan, Eur. Phys. J. B **39**, 155 (2004).
- [42] S. Greschner, M. Piraud, F. Heidrich-Meisner, I. P. McCulloch, U. Schollwöck, and T. Vekua, *Spontaneous increase of magnetic flux and chiral-current reversal in bosonic ladders: Swimming against the tide*, arXiv:1504.06564 (2015).
- [43] M. H. Devoret, A. Wallraff, and J. M. Martinis, *Superconducting Qubits: A Short Review*, eprint arXiv:cond-mat/0411174 (2004).
- [44] J. Q. You and F. Nori, Physics Today **58**, 42 (2005).
- [45] Note that the momentum distribution is a gauge dependent quantity, and that our gauge choice differs from the one of [6].

Supplemental Material for “Persisting Meissner state and incommensurate phases of hard-core boson ladders in a flux”

Supplementary material for “Incommensurate phases of a hard-core boson two-leg ladder in a flux”

CORRELATION FUNCTIONS AND OBSERVABLES IN BOSONIZATION

Bosonized Hamiltonian and observables

Let us first consider a single leg σ in the case of $\Omega = 0, \lambda = 0$. Hard core bosons are mapped on non-interacting spinless fermions by the Jordan-Wigner transformation[S1]. These non-interacting spinless fermions are then bosonized[S2]. The bosonized form of the Hamiltonian H_{\parallel} reads:

$$H_{\parallel} = \sum_{\sigma} \int \frac{dx}{2\pi} \left[uK(\pi\Pi_{\sigma})^2 + \frac{u}{K}(\partial_x\phi_{\sigma})^2 \right], \quad (\text{S1})$$

where $[\phi_{\sigma}(x), \Pi'_{\sigma}(x')] = i\delta_{\sigma\sigma'}\delta(x-x')$ and $\pi \int^x \Pi_{\alpha} = \theta_{\alpha}$. in Eq. (S3), u is the velocity of excitations, while K is the Tomonaga-Luttinger (TL) parameter. For non-interacting spinless fermions, $K = 1$ and $u = 2ta \sin(\pi n/2)$, where $n = \langle n_{\uparrow} + n_{\downarrow} \rangle$ is the average number of bosons per site and a is the lattice spacing. At half-filling (*i. e.* $n = 1$) $u = 2t$. The boson annihilation operators are represented as[S3][S2]:

$$b_{j,\sigma} = e^{i\theta_{\sigma}(ja)} \left[A_0 + \sum_{m \neq 0} A_m e^{2im(\phi(ja) - \pi \langle n_{\sigma} \rangle x/a)} \right]. \quad (\text{S2})$$

In the presence of a vector potential along the legs of the ladder, the lattice Hamiltonian can be brought back to the case of $\lambda = 0$ by the canonical transformation $b_{j,\sigma} = e^{-ij\lambda\sigma} \bar{b}_{j,\sigma}$. The bosonization technique can then be applied to the Hamiltonian written in terms of the $\bar{b}_{j,\sigma}$ bosons. One finds a Hamiltonian of the form (S1) with $\bar{\theta}_{\sigma}, \bar{\phi}_{\sigma}$ replacing $\theta_{\sigma}, \phi_{\sigma}$. Using Eq. (S2), one obtains $\theta(x) = \bar{\theta}(x) - \lambda\sigma x/a$, and $\phi(x) = \bar{\phi}(x)$ giving the bosonized Hamiltonian

$$H_{\parallel} = \sum_{\sigma} \int \frac{dx}{2\pi} \left[uK \left(\pi\Pi_{\sigma} + \sigma \frac{\lambda}{a} \right)^2 + \frac{u}{K}(\partial_x\phi_{\sigma})^2 \right], \quad (\text{S3})$$

Actually, it is convenient to turn to symmetric (*c*) and antisymmetric (*s*) representation, $\phi_{c,s} = \frac{\phi_{\uparrow} \pm \phi_{\downarrow}}{\sqrt{2}}$, $\theta_{c,s} = \frac{\theta_{\uparrow} \pm \theta_{\downarrow}}{\sqrt{2}}$, so that the full Hamiltonian reads:

$$H = H_c + H_s^{\lambda} \quad (\text{S4})$$

$$H_c = \int \frac{dx}{2\pi} \left[u_c K_c (\pi\Pi_c)^2 + \frac{u_c}{K_c} (\partial_x\phi_c)^2 \right] \quad (\text{S5})$$

$$H_s^{\lambda} = \int \frac{dx}{2\pi} \left[u_s K_s \left(\pi\Pi_s + \frac{\lambda}{a\sqrt{2}} \right)^2 + \frac{u_s}{K_s} (\partial_x\phi_s)^2 \right] \quad (\text{S6})$$

where $u_c K_c = u_s K_s = uK$, $u_c/K_c = u_s/K_s = u/K$, and we have used $\sigma = \pm 1/2$.

The boson annihilation operators become:

$$b_{j\sigma} = e^{\frac{i}{\sqrt{2}}(\theta_c + 2\sigma\theta_s)} \left[\sum_m A_m e^{im(\sqrt{2}\phi_c + 2\sigma\sqrt{2}\phi_s - 2\pi \langle n_{\sigma} \rangle x/a)} \right] \quad (\text{S7})$$

Therefore,

$$\langle b_{j\sigma} b_{0\sigma}^{\dagger} \rangle \sim \langle e^{\frac{i}{\sqrt{2}}\theta_c(ja)} e^{-\frac{i}{\sqrt{2}}\theta_c(0)} \rangle \langle e^{\frac{i}{\sqrt{2}}\sigma\theta_s(ja)} e^{-\frac{i}{\sqrt{2}}\sigma\theta_s(0)} \rangle + \dots \quad (\text{S8})$$

Using instead the bosonized expression for the density $\rho_{\sigma} = \frac{\langle n_{\sigma} \rangle}{a} - \partial_x\phi_{\sigma} + B_1 \sin(2\phi_{\sigma} - 2\pi \langle n_{\sigma} \rangle x/a)$ one obtains the the total boson density $\rho_{tot} = \rho_{\uparrow} + \rho_{\downarrow}$ as:

$$\rho_{tot}(x) = \frac{1}{a} - \frac{\sqrt{2}}{\pi} \partial_c\phi_c + 2B_0 e^{i\pi \frac{x}{a}} \sin \sqrt{2}\phi_c \cos \sqrt{2}\phi_s, \quad (\text{S9})$$

and the antisymmetric density $\sigma^z = (\rho_\uparrow - \rho_\downarrow)/2$ as:

$$\sigma^z(x) = -\frac{1}{\pi\sqrt{2}}\partial_x\phi_s + B_0 e^{i\pi\frac{x}{a}} \cos\sqrt{2}\phi_c \sin\sqrt{2}\phi_s, \quad (\text{S10})$$

where we have assumed $\langle n_\sigma \rangle = 1/2$. Now, if we turn on the interchain hopping Ω , we will obtain with the help of (S2) the following bosonized form:

$$H_{trans.} = \frac{2\Omega}{\alpha} \int dx \cos\sqrt{2}\theta_s [A_0^2 + 2A_1^2 \cos\sqrt{8}\phi_c + 2A_1^2 \cos\sqrt{8}\phi_s + \dots], \quad (\text{S11})$$

where \dots stands for less relevant operators. It is important to note that in a renormalization group calculation, operators $\cos\sqrt{8}\phi_c$ and $\cos\sqrt{8}\phi_s$ are generated in the flow. Since we are in the half-filled case, $\langle n_\uparrow + n_\downarrow \rangle = 1$, umklapp scattering $\cos\sqrt{8}\phi_c$ is present[S4, S5] and opens a gap in the c modes.

For $\langle n_\uparrow \rangle = \langle n_\downarrow \rangle$, the term $\cos\sqrt{8}\phi_\sigma$ is present, but is marginally irrelevant for repulsive interactions.

We have in the ground state $\langle \phi_c \rangle = 0$. Using Eqs. (S9), the staggered and uniform components of the total density have exponentially decaying correlations. Meanwhile, the antisymmetric density (S10) has a simplified expression for distances much larger than u_c/Δ_c where one can replace $\cos\sqrt{2}\phi_c$ by its average.

Besides density waves, the system can also present bond ordering. The bond order wave order parameter O_{BOW}^σ for spin σ boson is defined by:

$$b_{j+1,\sigma}^\dagger b_{j,\sigma} + b_{j,\sigma}^\dagger b_{j+1,\sigma} = T(ja) + (-)^j O_{BOW}^\sigma(ja), \quad (\text{S12})$$

where T is the kinetic energy density, and in bosonization

$$O_{BOW}^\sigma = C_0 \cos(2\phi_\sigma) \quad (\text{S13})$$

We can define the two order parameters:

$$O_{BOW}^c = \sum_\sigma O_{BOW}^\sigma = 2C_0 \cos\sqrt{2}\phi_c \cos\sqrt{2}\phi_s \quad (\text{S14})$$

$$O_{BOW}^s = \sum_\sigma \text{sign}(\sigma) O_{BOW}^\sigma = 2C_0 \sin\sqrt{2}\phi_c \sin\sqrt{2}\phi_s \quad (\text{S15})$$

In a Mott phase, O_{BOW}^s is always short range ordered, while $O_{BOW}^c \sim \cos\sqrt{2}\phi_s$. If we consider the real space Green's functions for the bosons, due to the long range order of ϕ_c , the exponentials $e^{i\beta\theta_c}$ of the dual field are short range ordered, and the boson Green's functions decay exponentially. Excitations of the total density are solitons and antisolitons of topological charge $\phi_c(+\infty) - \phi_c(-\infty) = \pm\pi/\sqrt{2}$. Such an excitation corresponds to a change of particle number ± 1 , and for fixed particle number density excitations are formed of soliton/antisoliton pairs.

For $\lambda = 0$, the term $2\Omega A_0^2 \cos\sqrt{2}\theta_s$ is a relevant perturbation with scaling dimension $1/(2K_s)$, opening a gap $\Delta_s \sim \Omega^{2K_s/(4K_s-1)}$ in the antisymmetric sector. We have in the ground state $\langle \theta_\sigma \rangle = \pi/\sqrt{2}$ and as a result all the fields $e^{i\beta\phi_\sigma}$ are short range ordered. Therefore, in the Mott-Meissner phase, all the density wave and bond order wave order parameters are short range ordered. Because of the long range order of θ_s we expect that the correlation functions $\langle b_{j,\sigma} b_{l,-\sigma}^\dagger \rangle$ are non-zero. A more precise estimate of the gap (albeit without log corrections) can be obtained from the results of [S6, S7]. Using these results, we predict that the soliton mass Δ_s behaves as:

$$\Delta_s = \frac{u_s}{a} \frac{2\Gamma\left(\frac{1}{8K_s-2}\right)}{\sqrt{\pi}\Gamma\left(\frac{2K_s}{4K_s-1}\right)} \left(\frac{\pi\Gamma\left(1 - \frac{1}{4K_s}\right)}{\Gamma\left(\frac{1}{4K_s}\right)} \frac{\Omega A_0^2 a}{u_s} \right)^{\frac{2K_s}{4K_s-1}}, \quad (\text{S16})$$

and the soliton/antisoliton dispersion is $E_s(k) = \sqrt{(u_s k)^2 + \Delta_s^2}$. In the case of hard core bosons, we have to set $K_s = 1$ in Eq.(S16). In such case, besides the solitons and antisolitons, there are two breathers[S8-S10], a light breather of mass Δ_s and a heavy breather of mass $\sqrt{3}\Delta_s$. The topological charge of the θ_s solitons/antisolitons is $\theta_s(+\infty) - \theta_s(-\infty) = \pm\pi\sqrt{2}$. The solitons therefore carry a spin current $u_s K_s$. In the case where one is considering the gap between the ground state and an excited state of total spin current zero (i. e. containing at least one soliton and one antisoliton), the measured gap will be $2\Delta_s$. The amplitude A_0 can be estimated for hard core bosons in the case of half-filling.[S11]

$$A_0^2 = 2^{1/6} e^{1/2} A^{-6}, \quad (\text{S17})$$

where $A \simeq 1.282427$ is Glaisher's constant. Using (S16) with $K_s = 1$ and (S17), we find:

$$\Delta_s = \frac{u_s}{a} \frac{2\Gamma(1/6)}{\sqrt{\pi}\Gamma(2/3)} \left(\frac{2^{1/6} e^{1/2} A^{-6} \Gamma(3/4) \pi \Omega a}{\Gamma(1/4)} \frac{1}{u_s} \right)^{2/3}, \quad (\text{S18})$$

for half-filling. Using $u_s = 2ta$, we finally have $\Delta_s/t = 3.3896(\Omega/t)^{2/3}$. The marginally irrelevant operator $\cos \sqrt{8}\phi_s$ can give rise to logarithmic corrections to that scaling[S12, S13] of the form $\Delta_s \sim \Omega^{2/3} |\ln \Omega|^{1/6}$.

Commensurate Incommensurate transition

Neglecting the marginally irrelevant term $\cos \sqrt{8}\phi_s$ as in [S14], the Hamiltonian (S6) (S11) describes the C-IC transition[S15–S17]. When λ exceeds the threshold $\lambda_c \sim (\Omega A_0^2 a / u_s)^{2-1/(2K_s)}$, it becomes energetically favorable to populate the ground state with a finite density of solitons of the field θ_s to form a Tomonaga-Luttinger liquid (TLL) of solitons. The low energy properties of that TLL are described by the effective Hamiltonian:

$$H^* = \int \frac{dx}{2\pi} \left[u_s^*(\lambda) K_s^*(\lambda) (\pi \Pi_s^*)^2 + \frac{u_s^*(\lambda)}{K_s^*(\lambda)} (\partial_x \phi)^2 \right], \quad (\text{S19})$$

and we have $\pi \Pi_s(x) = \pi \Pi_s^*(x) - q(\lambda)/\sqrt{2}$; $\theta_s(x) = \theta_s^*(x) - q(\lambda)x/\sqrt{2}$. Near the transition point λ_c , we have $q(\lambda) \sim C\sqrt{\lambda - \lambda_c}$. Moreover, as $\lambda \rightarrow \lambda_c + 0$, $K_s^*(\lambda)$ goes to a limiting value $K_s^{(0)}$ such that[S17, S18] the scaling dimension of $\cos \sqrt{2}\theta_s$ becomes 1. Since the scaling dimension of $\cos \sqrt{2}\theta_s$ with a Hamiltonian of the form (S19) is $1/[2K_s^*(\lambda)]$ we have $K_s^*(\lambda \rightarrow \lambda_c + 0) = 1/2$. Using a fermionization method[S14], an explicit form of $q(\lambda)$ can be obtained for $K_s = 1/2$.

The antisymmetric leg current (or screening current) operator

$$J_s(j) = -it \sum_{\sigma} \left(\sigma e^{i\lambda\sigma} b_{j,\sigma}^{\dagger} b_{j+1,\sigma} - \sigma e^{-i\lambda\sigma} b_{j+1,\sigma}^{\dagger} b_{j,\sigma} \right), \quad (\text{S20})$$

is obtained by differentiating the Hamiltonian with respect to the parameter λ . One finds:

$$J_s(x) = \frac{u_s K_s}{\pi \sqrt{2}} \left(\pi \Pi_s + \frac{\lambda}{a \sqrt{2}} \right) \quad (\text{S21})$$

In the Meissner phase, $\langle \Pi_s \rangle = 0$ so that:

$$\langle J_s \rangle = \frac{u_s K_s}{2\pi} \lambda \quad (\text{S22})$$

In the vortex phase, $J_s = u_s K_s (\lambda - \text{sign}(\lambda)q(\lambda))/(2\pi)$. By fermionization[S14], $q(\lambda) = \sqrt{\lambda^2 - \lambda_c^2}$ is obtained for $K_s = 1/2$.

In the Mott-Vortex state, we obtain the rung current as:

$$j_{\perp}(x) = \Omega A_0^2 \sin[\sqrt{2}\theta_s^*(x) - q(\lambda)x]. \quad (\text{S23})$$

In both the Meissner and the vortex phase, its expectation value $\langle j_{\perp} \rangle = 0$ vanishes. In the Meissner phase, the conversion current correlation function $C(x) = \langle j_{\perp}(x) j_{\perp}(0) \rangle$ decays exponentially whereas in the vortex phase:

$$C(x) = \frac{1}{2} (\Omega A_0^2)^2 \left(\frac{a^2}{x^2 + a^2} \right)^{\frac{1}{2K_s^*}} \cos[q(\lambda)x] \quad (\text{S24})$$

For $K_s^* = 1/2$, the Fourier transform:

$$C(k) = \frac{a(\Omega A_0^2)^2}{4} (e^{-|k-q(\lambda)|a} + e^{-|k+q(\lambda)|a}), \quad (\text{S25})$$

has two cusps at $k = \pm q(\lambda)$. Peaks divergent with system size appear in $C(k)$ for $K_s^* > 1$.

We can also obtain the spin-spin and bond order correlation functions. In the Mott-Vortex phase, the fields $e^{i\beta\phi_\sigma}$ have quasi-long range order. As a result, we find that:

$$\langle O_{BOW}^c(x) O_{BOW}^c(0) \rangle = C_0^2 \langle (\cos \sqrt{2}\phi_c) \rangle^2 \left(\frac{a^2}{x^2 + a^2} \right)^{K_s^*/2} \quad (S26)$$

$$\langle \sigma^z(x) \sigma^z(0) \rangle = \frac{K_s}{4\pi^2} \frac{a^2 - x^2}{(x^2 + a^2)^2} + (-)^{\frac{\pi}{a}} B_0^2 \langle (\cos \sqrt{2}\phi_c) \rangle^2 \left(\frac{a^2}{x^2 + a^2} \right)^{K_s^*/2} \quad (S27)$$

If we turn to the Fourier transforms, we find that for $k \simeq 0$,

$$S(k) = \frac{K_s^* |k|}{4\pi} e^{-|k|a}, \quad (S28)$$

by using the integral $\int_{-\infty}^{\infty} \frac{dx e^{ikx}}{x^2 + a^2} = \frac{\pi}{a} e^{-|k|a}$. For $k \simeq \frac{\pi}{a}$ and $K_s^* < 1$, we find that the correlation functions $S(k)$ and $S_{BOW_c}(k)$ are divergent as:

$$S(k) \sim S_{bow}^c(k) \sim \left| k - \frac{\pi}{a} \right|^{K_s^* - 1}, \quad (S29)$$

and as a result a divergence going as $|ka|^{-1/2}$ is expected at the transition, while far from the transition $K_s^* \simeq 1$, giving only a weak power law or logarithmic divergence. For $K_s^* > 1$, both $S_s(k)$ and for $S_{bow}^c(k)$ remain finite in the vicinity of π/a .

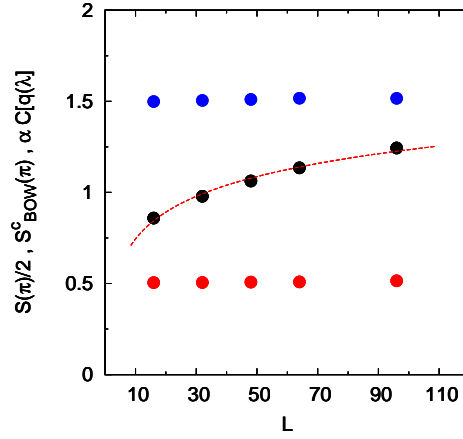


FIG. S1: Size dependence of $S(k = \pi)$ (red dots) and $S_{BOW}^c(k = \pi)$ (blue dots), for system sizes $L = 16, 32, 48, 64$ and 96 . Data are for $\Omega = 0.25$ and $\lambda = \pi/2$, well inside the vortex phase region. Both quantities don't show a visible size dependence in agreement with (S29) for $K_s^* = 1$. Solid black dots are $C(k = q(\lambda))\alpha$ with $\alpha = \Omega^2/16$ to be on the same scale on the graph. The size-scaling is compatible with a logarithmic dependence (red dotted line) as expected far from the transition region

If we turn to the momentum distribution, we will find:

$$\langle b_{j,\sigma} b_{l,\sigma'}^\dagger \rangle = \delta_{\sigma\sigma'} e^{-i\sigma q(\lambda)a(j-l)} \langle e^{i\theta_c(ja)/\sqrt{2}} e^{-i\theta_c(la)/\sqrt{2}} \rangle \langle e^{i\theta_s^*(ja)/\sqrt{2}} e^{-i\theta_s(la)/\sqrt{2}} \rangle \quad (S30)$$

$$= \delta_{\sigma\sigma'} e^{-i\sigma q(\lambda)a(j-l)} \frac{\langle e^{i\theta_c(ja)/\sqrt{2}} e^{-i\theta_c(la)/\sqrt{2}} \rangle}{(1 + (x/a)^2)^{1/(8K_s^*)}}. \quad (S31)$$

because of the exponential decay of the charge correlator, we expect that the momentum distribution of spin σ particles will be centered around $k = -\sigma q(\lambda)$. The total momentum distribution will thus have two peaks for $k = \pm q(\lambda)/2$.

INCOMMENSURATION FOR $\lambda \simeq \pi$

For λ close to π , the form (S6) for the Hamiltonian cannot be used as $\lambda u_s/a$ is not a small quantity compared with the energy cutoff u_s/a . To describe the low energy physics at $\lambda = \pi$, it is necessary to choose a gauge with the vector

potential along the rungs of the ladder, so that the interchain hopping reads:

$$H_{hop.} = \Omega \sum_j (-)^j b_{j,\sigma}^\dagger b_{j,-\sigma}, \quad (\text{S32})$$

Applying bosonization to (S32), we obtain the following representation for interchain hopping:

$$H_{hop.} = \frac{\Omega}{2\pi a} \int dx \cos \sqrt{2}\phi_c \left[e^{-i\sqrt{2}(\theta_s+\phi_s)} + e^{-i\sqrt{2}(\theta_s-\phi_s)} + e^{i\sqrt{2}(\theta_s+\phi_s)} + e^{i\sqrt{2}(\theta_s-\phi_s)} \right], \quad (\text{S33})$$

which can be rewritten in terms of $SU(2)_1$ Wess-Zumino-Novikov-Witten (WZNW) currents[S19]:

$$H_{hop.} = \Omega \int dx \cos \sqrt{2}\phi_c (J_R^y + J_L^y). \quad (\text{S34})$$

The resulting Hamiltonian $H_c + H_s + H_{hop.}$ can be treated in mean-field theory[S20–S23], giving:

$$H_{MF} = H_c^{MF} + H_s^{MF}, \quad (\text{S35})$$

$$H_c^{MF} = \int \frac{dx}{2\pi} \left[u_c K_c (\pi \Pi_c)^2 + \frac{u_c}{K_c} (\partial_x \phi_c)^2 \right] + \frac{g_c}{\pi a} \int dx \cos \sqrt{2}\phi_c, \quad (\text{S36})$$

$$H_s^{MF} = \frac{2\pi u_s}{3} \int dx (\mathbf{J}_R \cdot \mathbf{J}_R + \mathbf{J}_L \cdot \mathbf{J}_L) + h_s \int dx (J_R^y + J_L^y), \quad (\text{S37})$$

where:

$$\begin{aligned} \frac{g_c}{\pi a} &= 8\Omega \langle J_R^y + J_L^y \rangle_{s,MF}, \\ h_s &= 8\Omega \langle \cos \sqrt{2}\phi_c \rangle_{c,MF}. \end{aligned} \quad (\text{S38})$$

Using a $\frac{\pi}{2}$ rotation around the x axis, $J_\nu^y = \tilde{J}_\nu^z$, $J_\nu^z = -\tilde{J}_\nu^y$, and applying abelian bosonization[S24], we rewrite:

$$H_s^{MF} = \int \frac{dx}{2\pi} u_s \left[(\pi \tilde{\Pi}_s)^2 + (\partial_x \tilde{\phi}_s)^2 \right] - \frac{h_s}{\pi\sqrt{2}} \int \partial_x \tilde{\phi}_s dx, \quad (\text{S39})$$

which allows us to write:

$$-\frac{1}{\pi\sqrt{2}} \langle \partial_x \tilde{\phi}_s \rangle = \sum_{\nu=R,L} \langle \tilde{J}_\nu^z \rangle = \langle J_R^y + J_L^y \rangle = -\frac{h_s}{2\pi u_s}, \quad (\text{S40})$$

and allows us to solve (S38) with $h_s \sim \Omega^2$ and $g_c \sim \Omega^3$. We obtain a gap in the total density excitations, $\Delta_c \sim \Omega^2$, while the antisymmetric modes remain gapless and develop an incommensuration. To characterize the incommensuration, we need to detail the rotation of the $SU(2)_1$ WZNW currents and primary fields. After shifting $\tilde{\phi}_s \rightarrow \tilde{\phi}_s + \frac{h_s x}{u_s \sqrt{2}}$, we find:

$$-\frac{1}{\pi\sqrt{2}} \partial_x \phi_s = -\frac{1}{2\pi a} \sum_{r,r'=\pm} e^{ir\sqrt{2}(\tilde{\theta}_s+r'\tilde{\phi}_s)+irr'\frac{h_s x}{u_s}}, \quad (\text{S41})$$

$$\sum_{r=\pm} \sin \sqrt{2}(\theta_s + r\phi_s) = \sum_{r=\pm} \sin \sqrt{2} \left(\tilde{\theta}_s + r\tilde{\phi}_s + r\frac{h_s x}{u_s} \right), \quad (\text{S42})$$

$$\sum_{r=\pm} \cos \sqrt{2}(\theta_s + r\phi_s) = -\frac{1}{\pi\sqrt{2}} \partial_x \tilde{\phi}_s - \frac{h_s}{2\pi u_s}, \quad (\text{S43})$$

and:

$$\sin \sqrt{2}\theta_s = \sin \sqrt{2}\tilde{\theta}_s \quad (\text{S44})$$

$$\cos \sqrt{2}\theta_s = \sin \left(\sqrt{2}\tilde{\phi}_s + \frac{h_s x}{u_s} \right) \quad (\text{S45})$$

$$\sin \sqrt{2}\phi_s = -\cos \sqrt{2}\tilde{\theta}_s \quad (\text{S46})$$

$$\cos \sqrt{2}\phi_s = \cos \left(\sqrt{2}\tilde{\phi}_s + \frac{h_s x}{u_s} \right) \quad (\text{S47})$$

Since we have:

$$j_{\perp}(j) = \frac{\Omega}{\pi a} \sum_{r=\pm} \sin \sqrt{2}(\theta_s + r\phi_s) + \frac{2\Omega(-)^j}{\pi a} \sin \sqrt{2}\theta_s, \quad (\text{S48})$$

$$\sigma^z(x) = -\frac{1}{\pi\sqrt{2}} \partial_x \phi_s + \frac{(-1)^j}{\pi a} \langle \cos \sqrt{2}\phi_c \rangle \sin \sqrt{2}\phi_s, \quad (\text{S49})$$

$$O_{BOW}^c = \frac{(-1)^j}{\pi a} \langle \cos \sqrt{2}\phi_c \rangle \cos \sqrt{2}\phi_s \quad (\text{S50})$$

we find, after the rotation:

$$j_{\perp}(j) = \frac{\Omega}{\pi a} \sum_{r=\pm} \sin \sqrt{2} \left(\tilde{\theta}_s + r\tilde{\phi}_s + r\frac{h_s x}{u_s} \right) + \frac{2\Omega(-)^j}{\pi a} \sin \sqrt{2}\tilde{\theta}_s, \quad (\text{S51})$$

$$\sigma^z(x) = \frac{1}{\pi a} \sum_{r=\pm} \cos \sqrt{2} \left(\tilde{\theta}_s + r\tilde{\phi}_s + r\frac{h_s x}{u_s} \right) - \frac{(-1)^j}{\pi a} \langle \cos \sqrt{2}\phi_c \rangle \cos \sqrt{2}\tilde{\theta}_s, \quad (\text{S52})$$

$$O_{BOW}^c = \frac{(-1)^j}{\pi a} \langle \cos \sqrt{2}\phi_c \rangle \cos \left(\sqrt{2}\tilde{\phi}_s + \frac{h_s x}{u_s} \right) \quad (\text{S53})$$

so that:

$$\langle j_{\perp}(j)j_{\perp}(j') \rangle \sim \frac{1}{2\pi^2(j-j')^2} \cos \left(\frac{h_s(j-j')}{u_s} \right) + \frac{(-1)^{j-j'}}{|j-j'|}, \quad (\text{S54})$$

$$\langle \sigma^z(j)\sigma^z(j') \rangle \sim \frac{1}{2\pi^2(j-j')^2} \cos \left(\frac{h_s(j-j')}{u_s} \right) + \frac{(-1)^{j-j'}}{|j-j'|}, \quad (\text{S55})$$

$$\langle O_{BOW}^c(j)O_{BOW}^c(j') \rangle \sim \frac{(-1)^{j-j'}}{|j-j'|} \cos \left(\frac{h_s(j-j')}{u_s} \right) \quad (\text{S56})$$

We see that an incommensuration of wavevector $p(\Omega) = h_s/u_s$ develops in the $k \simeq 0$ component of the rung current and density wave correlations. Since $p(\Omega) \sim \Omega^2$ (see Fig. S2), the incommensuration increases with interchain hopping. The Fourier transform of the $k \simeq 0$ component behaves as $|k - p(\Omega)| + |k + p(\Omega)|$, i. e. it is constant for $|k| < p(\Omega)$ and linear in k for $|k| > p(\Omega)$.

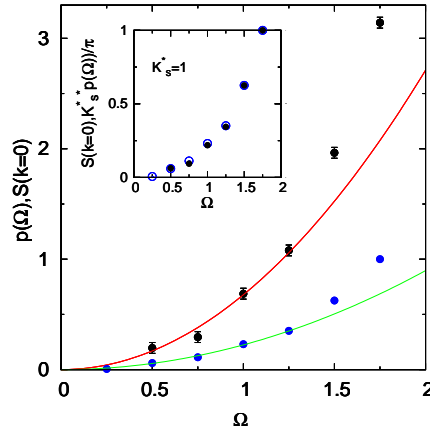


FIG. S2: A graph of the incommensuration $p(\Omega) = h_s/u_s$ at $\lambda = \pi$ obtained from numerical data ($L=64$ in PBC). The blue dots are the value of $S(k=0)$, while the black dots correspond to the slope discontinuity $k = p(\Omega)$. The red and green lines are quadratic fits. In the inset we show $S(k=0)$, open blue dots, together with the $K_s^* p(\Omega)/\pi$, black solid dots, with the choice $K_s^* = 1$

Since the boson annihilation operators do not correspond to primary fields of the $SU(2)_1$ WZNW model, we cannot directly derive their expression from $SU(2)$ symmetry. However, since $e^{i\theta_s/\sqrt{2}}$ has conformal dimensions $(1/16, 1/16)$

its expression in terms of $\tilde{\theta}_s$ and $\tilde{\phi}_s$ has to be a sum of operators of conformal dimensions (1/16, 1/16). A general expression is:

$$e^{i\frac{\theta_s}{\sqrt{2}}} = A_0 e^{i\frac{\tilde{\theta}_s}{\sqrt{2}}} + A_1 e^{i\frac{\tilde{\phi}_s}{\sqrt{2}}} + A_2 e^{-i\frac{\tilde{\theta}_s}{\sqrt{2}}} + A_3 e^{-i\frac{\tilde{\phi}_s}{\sqrt{2}}}. \quad (\text{S57})$$

Moreover, the operator product expansion:

$$e^{i\frac{\theta_s(x)}{\sqrt{2}}} e^{i\frac{\theta_s(x')}{\sqrt{2}}} = \left| \frac{x-x'}{a} \right|^{1/4} e^{i\sqrt{2}\theta_s(x)}, \quad (\text{S58})$$

has to be satisfied, so, for $\lambda = \pi$, we must have $\{A_k, A_j\} = \delta_{kj} e^{-ik\frac{\pi}{4}}$ which can be satisfied by writing A_k as the product of a 4×4 Dirac matrix[S25] by a phase $e^{-ik\frac{\pi}{4}}$. In the case of $\lambda = \pi$ we obtain the correlator:

$$\langle e^{i\frac{\theta_s(x)}{\sqrt{2}}} e^{-i\frac{\theta_s(x')}{\sqrt{2}}} \rangle = \left(\frac{a}{|x-x'|} \right)^{\frac{1}{4}} \left[2 + 2 \cos \frac{h_s}{u_s} (x-x') \right], \quad (\text{S59})$$

where the cos results from the correlation of the $e^{\pm i\tilde{\phi}_s/\sqrt{2}}$. This implies that the momentum distribution is:

$$n_\sigma(k) = \int dx e^{i(k+\pi\sigma)x} \langle e^{-i\frac{\theta_s(x)}{\sqrt{2}}} e^{i\frac{\theta_s(0)}{\sqrt{2}}} \rangle \langle e^{i\frac{\theta_s(x)}{\sqrt{2}}} e^{-i\frac{\theta_s(0)}{\sqrt{2}}} \rangle \quad (\text{S60})$$

$$= \int dx e^{i(k+\pi\sigma)x} \langle e^{-i\frac{\theta_s(x)}{\sqrt{2}}} e^{i\frac{\theta_s(0)}{\sqrt{2}}} \rangle \left(\frac{a}{|x|} \right)^{\frac{1}{4}} \left[2 + 2 \cos \frac{h_s x}{u_s} \right] \quad (\text{S61})$$

$$= \nu(k + \pi\sigma) + \frac{1}{2}\nu \left(k + \pi\sigma + \frac{h_s}{u_s} \right) + \frac{1}{2}\nu \left(k + \pi\sigma - \frac{h_s}{u_s} \right), \quad (\text{S62})$$

where:

$$\nu(k) = \int dx e^{ikx} \langle e^{-i\frac{\theta_s(x)}{\sqrt{2}}} e^{i\frac{\theta_s(0)}{\sqrt{2}}} \rangle \left(\frac{a}{|x|} \right)^{\frac{1}{4}}. \quad (\text{S63})$$

Since the width at half maximum of the Lorentzian-shaped graph of the function ν scales as $\Delta_c/u_c \sim \Omega^2$ and $h_s/u_s \sim \Omega^2$, the graph of $n(k)$ can either comprise 3 peaks or a single broad peak centered in $\pi\sigma$ depending on the dimensionless ratio $h_s u_c / (u_s \Delta_c)$.

When $\lambda < \pi$, we choose a gauge such that:

$$\begin{aligned} H &= -t \sum_{j,\sigma} \left(b_{j,\sigma}^\dagger e^{i(\lambda-\pi)\sigma} b_{j+1,\sigma} + \text{H.c.} \right) \\ &+ \Omega \sum_{j,\sigma} (-1)^j b_{j,\sigma}^\dagger b_{j,-\sigma}, \end{aligned} \quad (\text{S64})$$

and we define $\delta\lambda = \lambda - \pi$. The mean field Hamiltonian becomes $H_{MF} = H_c^{MF} + H_s^{MF}$ with:

$$H_s^{MF} = \frac{2\pi u_s}{3} \int dx (\mathbf{J}_R \cdot \mathbf{J}_R + \mathbf{J}_L \cdot \mathbf{J}_L) + h_s \int dx (J_R^y + J_L^y) + \frac{u_s \delta\lambda}{a} \int dx (J_R^z - J_L^z), \quad (\text{S65})$$

and H_c^{MF} unchanged. We now have to make a different rotation around x for the right moving and the left moving current:

$$J_R^y = \sin \varphi \tilde{J}_R^y + \cos \varphi \tilde{J}_R^z \quad (\text{S66})$$

$$J_R^z = -\cos \varphi \tilde{J}_R^y + \sin \varphi \tilde{J}_R^z \quad (\text{S67})$$

$$J_L^y = -\sin \varphi \tilde{J}_L^y + \cos \varphi \tilde{J}_L^z \quad (\text{S68})$$

$$J_L^z = -\cos \varphi \tilde{J}_L^y + \sin \varphi \tilde{J}_L^z \quad (\text{S69})$$

To find;

$$H_s^{MF} = \int \frac{dx}{2\pi} u_s \left[(\pi \tilde{\Pi}_s)^2 + (\partial \tilde{\phi}_s)^2 \right] - \frac{h_s(\lambda)}{\pi\sqrt{2}} \int \partial_x \tilde{\phi}_s dx, \quad (\text{S70})$$

where $h_s(\lambda) = \sqrt{h_s^2 + u_s^2(\delta\lambda/a)^2}$. We still have $\langle J_R^y + J_L^y \rangle = -\frac{h_s}{2\pi u_s}$, so the mean-field equations remain the same. We also find:

$$\sin \sqrt{2}\theta_s = \frac{h_s}{h_s(\lambda)} \sin \sqrt{2}\tilde{\theta}_s + \frac{u\delta\lambda/a}{h_s(\lambda)} \cos \left(\sqrt{2}\tilde{\phi}_s + \frac{h_s(\lambda)}{u_s}x \right) \quad (\text{S71})$$

$$\cos \sqrt{2}\theta_s = \sin \left(\sqrt{2}\tilde{\phi}_s + \frac{h_s(\lambda)}{u_s}x \right) \quad (\text{S72})$$

$$\sin \sqrt{2}\phi_s = -\cos \sqrt{2}\tilde{\theta}_s \quad (\text{S73})$$

$$\cos \sqrt{2}\phi_s = \frac{h_s}{h_s(\lambda)} \cos \left(\sqrt{2}\tilde{\phi}_s + \frac{h_s(\lambda)}{u_s}x \right) - \frac{u\delta\lambda/a}{h_s(\lambda)} \sin \sqrt{2}\tilde{\theta}_s \quad (\text{S74})$$

The staggered part of the rung current correlations becomes:

$$\langle j_\perp(x)j_\perp(0) \rangle \sim \frac{(-)^{x/a}}{|x|} \frac{h_s^2 + \left(\frac{u_s\delta\lambda}{a}\right)^2 \cos \frac{h_s(\lambda)}{u_s}x}{h_s(\lambda)^2}, \quad (\text{S75})$$

so that the Fourier transform will present peaks at $k = \frac{\pi}{a}$ and $k = \frac{\pi}{a} \pm h_s(\lambda)/u_s$. When $\delta\lambda$ is increased, the two peaks at $k = \frac{\pi}{a} \pm \frac{h_s(\lambda)}{u_s}$ become dominant, and we crossover to the behavior already discussed for weak λ . In the case of $S(k)$, the peak at $k = \pi$ is not split as λ is reduced. If we look at the BOW^c correlations, a peak at $k = \pi$ appears, and becomes the dominant peak when $\delta\lambda$ is increased. Using the rotation (S66) we can also obtain the antisymmetric density correlations as:

$$\frac{1}{2\pi^2} \langle \partial_x \phi_s(x) \partial_x \phi_s(0) \rangle = \frac{1}{2\pi^2 x^2} \left[\frac{\left(\frac{u_s\delta\lambda}{a}\right)^2}{h_s^2(\lambda)} + \frac{h_s^2}{h_s^2 + \left(\frac{u_s\delta\lambda}{a}\right)^2} \cos(h_s(\lambda)/u_s x) \right] \quad (\text{S76})$$

When $\delta\lambda$ increases, this expression crosses over to the $1/(2\pi^2 x^2)$ which was obtained at small λ . $S(k)$ now presents a change of slope at $|k| = h_s(\lambda)/u_s$.

As to the $k \simeq 0$ component of the rung current, since it is proportional to $J_R^x + J_L^x$ it becomes $\tilde{J}_R^x + \tilde{J}_L^x$ under the rotation, and the correlator becomes:

$$\frac{1}{2\pi^2(j-j')^2} \cos \left(\frac{h_s(\lambda)}{u_s}(j-j') \right), \quad (\text{S77})$$

-
- [S1] P. Jordan and E. Wigner, *Z. Phys.* **47**, 631 (1928).
[S2] T. Giamarchi, *Quantum Physics in One Dimension* (Oxford University Press, Oxford, 2004).
[S3] F. D. M. Haldane, *Phys. Rev. Lett.* **47**, 1840 (1981).
[S4] P. Donohue and T. Giamarchi, *Phys. Rev. B* **63**, 180508(R) (2001).
[S5] F. Crépin, N. Laflorencie, G. Roux, and P. Simon, *Phys. Rev. B* **84**, 054517 (2011).
[S6] A. B. Zamolodchikov, *Int. Review of Modern Physics A* **10**, 1125 (1995).
[S7] S. Lukyanov and A. B. Zamolodchikov, *Nucl. Phys. B* **493**, 571 (1997).
[S8] G. S. Uhrig and H. J. Schulz, *Phys. Rev. B* **54**, R9624 (1996).
[S9] I. Affleck, *Nucl. Phys. B* **265**, 448 (1986).
[S10] A. M. Tsvelik, *Phys. Rev. B* **45**, 486 (1992).
[S11] A. A. Ovchinnikov, *Journal of Physics Condensed Matter* **16**, 3147 (2004), arXiv:math-ph/0311050.
[S12] M. Oshikawa and I. Affleck, *Phys. Rev. Lett.* **79**, 2883 (1997).
[S13] I. Affleck and M. Oshikawa, *Phys. Rev. B* **60**, 1039 (1999), *phys. Rev. B* **62**, 9200(E) (2000).
[S14] E. Orignac and T. Giamarchi, *Phys. Rev. B* **64**, 144515 (2001), cond-mat/0011497.
[S15] G. I. Japaridze and A. A. Nersesyan, *JETP Lett.* **27**, 334 (1978).
[S16] V. L. Pokrovsky and A. L. Talapov, *Phys. Rev. Lett.* **42**, 65 (1979).
[S17] H. J. Schulz, *Phys. Rev. B* **22**, 5274 (1980).
[S18] R. Chitra and T. Giamarchi, *Phys. Rev. B* **55**, 5816 (1997).
[S19] A. Tsvelik, *Quantum Field Theory in Condensed Matter Physics* (Cambridge University Press, Cambridge, 1995).
[S20] A. A. Nersesyan, A. O. Gogolin, and F. H. L. Essler, *Phys. Rev. Lett.* **81**, 910 (1998).
[S21] P. Lecheminant, T. Jolicoeur, and P. Azaria, *Phys. Rev. B* **63**, 174426 (2001).
[S22] T. Jolicoeur and P. Lecheminant, *Prog. Theor. Phys. Supp.* **145**, 23 (2002).
[S23] M. Zarea, M. Fabrizio, and A. Nersesyan, *Eur. Phys. J. B* **39**, 155 (2004).
[S24] A. Nersesyan, A. Luther, and F. Kusmartsev, *Phys. Lett. A* **176**, 363 (1993).
[S25] C. Itzykson and J. B. Zuber, *Quantum Field Theory* (Mc Graw Hill, New-York, 1980).

